

ORIGINAL ARTICLE

Open Access



Effects of Prestressing of the Ring Gear in Interference Fit on Flexural Fatigue Strength of Tooth Root

Shiping Yang*, Yixing Ji, Yulin Mo and Tianyu Xia

Abstract

When the gearbox body interference is connected to the ring gear, prestressing occurs in the ring gear, which has a significant impact on the strength and life of the gear. Research on the prestressing of the inner ring gear is in the preliminary stage, and the distribution rule of the prestressing and the influence of each parameter on the interference prestressing have not been derived. In this paper, based on the method of calculating the prestressing of the thick cylinder in interference fit, the ring gear is found to be equivalent to a thick cylinder, and the distribution rule of prestressing of the ring gear in the interference fit is inferred. Then, by modeling and analyzing the gearbox body and ring gear in the interference fit using ABAQUS, the distribution rule of prestressing the ring gear in the interference fit is obtained through a numerical simulation. Finally, the prestressing of the ring gear in the interference fit is measured using X-ray diffraction, and the distribution rule of prestressing of the ring gear in the interference fit is obtained through analysis. Compared with the distribution rule of prestressing in theory, numerical simulation, and experiment, the theoretical distribution rule of prestressing is amended through a statistical method, and a more accurate formula of prestressing is obtained. Through the calculation of the stress and bending moment in the dangerous section of the ring gear through prestressing, the formula for checking the tooth root flexural fatigue strength in the interference fit prestressing is inferred. This research proposes a tooth root bending strength conditional formula for the inner ring gear of the interference fit, which serves as a guide for the design and production of the actual interference joint inner ring gear.

Keywords: Interference fit, Ring gear, Prestressing, Tooth root flexural fatigue strength, X-ray diffraction (XRD)

1 Introduction

The interference fit is a method in which a container and contained item is fastened based on the magnitude of interference [1, 2]. In a planetary gear reducer [3], wind power gearbox [4], and other transmissions, owing to the requirements of the structure, the ring gear is always manufactured on the gearbox [5]. Thus, the material of the gearbox needs to be same as that of the ring gear, which increases the cost of the gearbox. If the gearbox is assembled with a ring gear in the interference fit, the gearbox can be processed using a common casting

material, reducing costs and enhancing the market competitiveness of these transmissions.

Prestressing occurs in the ring gear through the gearbox interference fit with the ring gear, which impacts the tooth root flexural fatigue strength of the gear. Therefore, it is necessary to calculate the prestressing of the ring gear in the interference fit, consider the effect on the dangerous tooth root section of the ring gear, and correct the formula of tooth root flexural fatigue strength. Among the research conducted on interference fit of a gear and its prestressing, Jiang et al. [6] calculated the prestressing of the gear and ring in the interference fit based on a VK-63 gearing speed-up device. Based on a crankshaft gear, which is interference-fitted in the engine, Zou et al. [7] determined the relationship between the inner diameter of the gear, the magnitude of interference, and the

*Correspondence: yspxtu@163.com
School of Mechanical Engineering, Xiangtan University, Xiangtan 411105, China

prestressing. Yan et al. [8] established the distribution rule of prestressing of the gear in the interference fit. Zhu [9] based on ANSYS, analyzed the relationship of the interference between the keyless joint and the maximum prestressing; Zhao et al. [10] based on ANSYS, built the prestressed mode of the planetary gear train of the transmission; Wang [11] analyzed the influence of prestressing on interference fit of dump truck axle; Kim et al. [12] simulated the hot assembly procedure of the external gear and axis in the interference fit, and predicted the amount of deformation of the teeth profiles, considering the shrink-fitting load and amount of expansion of the gear with major process variables, and the amount of shrink-fitting interference; Rahman et al. [13] established the relationship between the friction coefficient and the stress of the contact area by studying the shaft and bushing of the interference joint; Hao et al. [14] studied the contact stress of the interference fit of the planetary carrier based on the finite element method; and Frederic et al. [15] obtained the reduction coefficient of the fretting fatigue strength of the interference joint. These studies have proposed effective calculation methods for the design of interference fit gear or similar joints. At the same time, a comprehensive analysis of the effects of prestressing and contact stress on the gear teeth of the interference coupling gear was made. However, the calculation formula for the prestressing of the gear interference joint, especially the ring gear, has not mentioned nor derived.

Prestressing analysis of the interference fit is extremely complex, and a simple theoretical analysis cannot meet the requirements [16]. With further engineering applications, the finite element method [17, 18] and trial method have been applied to the analysis of prestressing in an interference fit, and these methods can determine the distribution rule of prestressing of the gear in the interference fit more accurately.

This paper is based on XE82 and XE93 yaw pitch reducers [19, 20]. Focusing on the research target, the distribution rule of prestressing of the gearbox interference fits with the ring gear in the elastic range are first deduced, and the theoretical curves of the internal gear in the interference fit of prestressing are drawn up. Then, the simulation curves of the prestressing of the ring gear in the interference fit are analyzed using ABAQUS. The prestressing of the ring gear in the interference fit is measured through X-ray diffraction (XRD); the distribution rule of the prestressing of the ring gear in the interference fit is obtained through an analysis; and the trial curves of the prestressing of the ring gear in the interference fit are obtained. By comparing the distribution rule of prestressing of the theoretical curve, the simulation, and the trial curve, the accuracy of the prestressing formula of the

ring gear in the interference fit is verified. Finally, according to the calculation formulas of the tooth root bending fatigue strength, the meshing load of the ring gear and the prestressing of the interference fit in the dangerous section are synthesized. Then, the formula for checking the tooth root flexural fatigue strength is obtained, which can guide the design of the gearbox in the interference fit.

2 Mathematical Model of Prestressing of the Ring Gear in Interference Fit

In the calculation of the flexural fatigue strength of the tooth root, the gear is always regarded as a cantilever beam [21], and the location of the dangerous section is determined using a 30° tangent method. In a wind power planetary gear reducer, the ring gear is born not only by the meshing load of the planetary gear, but also the prestressing σ_t of the interference fitting when the gearbox body interference fits the ring gear. In a traditional thick cylinder, the formula of the prestressing of the inner cylinder in the interference fit is written as follows [22]:

$$\sigma_t = \frac{pr_2^2}{r_2^2 - r_1^2} \left(1 + \frac{r_1^2}{r_2^2} \right), \tag{1}$$

where r_1 is the radius of the inner cylinder, r_2 is the radius of the outer cylinder, and p is the interference fit stress. As can be seen from [22],

$$p = \frac{\delta}{d_f \left(\frac{C_a}{E_a} + \frac{C_i}{E_i} \right)}, \tag{2}$$

where d_f is the joint diameter, δ is the amount of interference, E_a is the outer cylinder material modulus of elasticity (MPa), E_i is the inner cylinder material modulus of elasticity (MPa), and C_a and C_i are the coefficients of the inner and outer cylinder, respectively. The formulas are shown as follows:

$$C_a = \frac{r_4^2 + r_f^2}{r_4^2 - r_f^2} + \nu_a, \tag{3}$$

$$C_i = \frac{r_f^2 + r_1^2}{r_f^2 - r_1^2} - \nu_i, \tag{4}$$

where r_1 is the inner radius of the inner cylinder (mm), r_f is the interference cylinder joint diameter (mm), r_4 is the outer radius of the outer cylinder (mm), ν_a is the Poisson's ratio of the outer cylinder, and ν_i is the Poisson's ratio of the inner cylinder.

Because the media of inner gear teeth are discontinuous, the inner cylinder is regarded as a thick cylinder, and

the pitch circle diameter of the inner gear is regarded as the inner diameter of the thick cylinder [23]. The prestressing formula of the ring gear in the interference fit is then determined as follows:

$$\begin{aligned} \sigma_t &= \frac{p \cdot r_i^2}{r_i^2 - r_r^2} \left(1 + \frac{r_r^2}{r^2} \right) \\ &= \frac{p \cdot r_i^2}{r_i^2 - r_r^2} + \frac{p \cdot r_i^2 \cdot r_r^2}{r_i^2 - r_r^2} \cdot \frac{1}{r^2} \\ &= A_1 + B_1 \cdot \frac{1}{r^2}, \end{aligned} \tag{5}$$

where r_i is the radius of the combined surface, and r_r is the radius of the inner gear's pitch circle.

Then, based on the calculation formula of prestressing σ_p , the theoretical curve of the prestressing of the ring gear in the interference fit is obtained, which is shown in Figure 1.

3 Design of Experimental Scheme

Based on the prestressing formula of the ring gear in the interference fit, the ring gear's modulus, the difference between the ring gear diameter and gear teeth diameter, the transmitted torque, and the combined length are chosen as the four key factors, and an orthogonal experiment on these four factors and three levels is conducted [24]. The models of the gearbox and ring gear in the interference fit are simulated and tested. The factor level table is obtained, as shown in Table 1.

Based on the orthogonal experiment on the four factors and three levels, the orthogonal table is obtained, as shown in Table 2.

Nine groups of experimental data were calculated, and the theoretical curves of the prestressing from

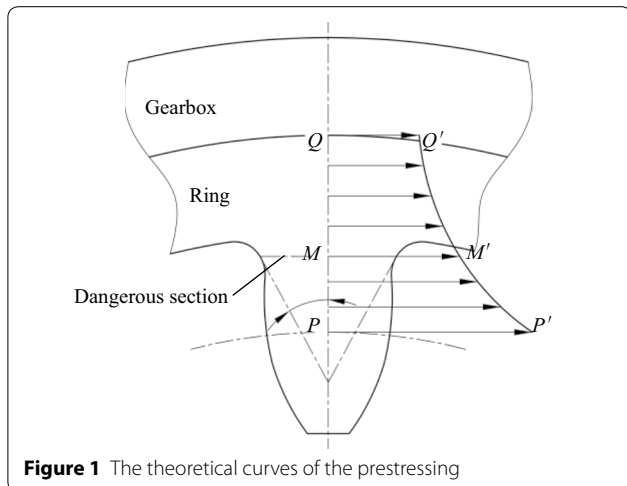


Figure 1 The theoretical curves of the prestressing

Table 1 Horizontal factor

Factors	Level 1	Level 2	Level 3
A Modulus of ring gear m (mm)	1	2	3
B Difference between outer diameter of ring gear and diameter of root circle d (mm)	10	20	30
C The transmitted torque M (N·m)	350	450	550
D The combined length L (mm)	20	40	60

experiments 1 through 9 are obtained. Then, the nine groups of experiments were simulated and tested, and the simulation curves and experimental curves of the prestressing were obtained.

What we desire is an arm exoskeleton which is capable of following the motions of the human upper-limb accurately, and supplying the human upper-limb with proper force feedback if needed. In order to achieve an ideal controlling performance, we have to examine the structure of the human upper-limb.

4 Simulation Based on ABAQUS

4.1 Modelling

The data from experiments 1 and 9 were chosen, and the ring gears and gearboxes were modelled using SolidWorks.

In experiment 1, the modulus of ring gear $m = 1$ mm, tooth numbers $z = 24$, pitch circle diameter $d_1 = 24$ mm, outer diameter $d = 46.5$ mm, and tooth width $b = 20$ mm. According to the transmitted torque M of experiment 1, the magnitude of interference δ is calculated, and the magnitude of interference $\delta = 0.059$ mm. The inner diameter of the gearbox $d_2 = 46.441$ mm, outer diameter $d_3 = 106.5$ mm, and length $l = 20$ mm.

In experiment 8, the modulus of the ring gear $m = 3$ mm, tooth numbers $z = 24$, pitch circle diameter $d_1 = 72$ mm, outer diameter $d = 119.5$ mm, and tooth width

Table 2 Orthogonal table

Experiment No.	Factors			
	A	B	C	D
1	1	10	350	20
2	1	20	450	40
3	1	30	550	60
4	2	10	450	60
5	2	20	550	20
6	2	30	350	40
7	3	10	550	40
8	3	20	350	60
9	3	30	450	20

$b = 60$ mm. According to the transmitted torque M of experiment 8, the magnitude of interference δ is calculated, and the magnitude of interference $\delta = 0.101$ mm. The inner diameter of the gearbox $d_2 = 119.399$ mm, outer diameter $d_3 = 179.5$ mm, and length $l = 60$ mm.

4.2 Meshing

Owing to the periodic symmetry of the ring gear and the box, in order to save computing resources and time, we intercept the 1/24 entity to build the model.

In ABAQUS, in order to ensure accurate calculation, the inner ring gear is divided into relatively fine hexahedral meshes. In order to improve the calculation efficiency, the box is divided into coarser meshes, and the unit type adopts the eight-node hexahedral linear reduction integral unit C3D8R. The finite element model in experiment 1 is divided into 14380 units and 16899 nodes. The finite element model in experiment 8 is divided into 149265 units and 160243 nodes.

The material of the ring gear is 42CrMoA, the elastic modulus $E = 206$ GPa, and Poisson's ratio $\nu = 0.3$. The material of the gearbox is QT450, the elastic modulus $E = 147$ GPa, and Poisson's ratio $\nu = 0.25$. The 1/24 solid model is meshed, and the grids of the ring gear are thinned. The mesh is shown in Figure 2.

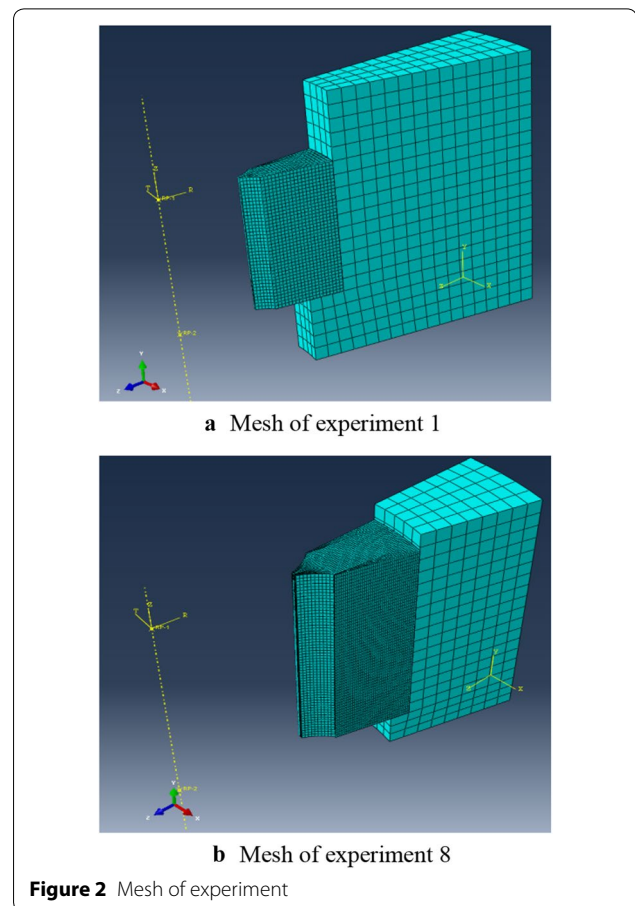
4.3 Contact and Boundary Conditions

The contact between the box and the ring gear is set to face-to-face contact. Since the prestress of the inner ring gear interference fit is the focus of this study, the mesh size of the inner ring gear is finer, so the inner surface of the box is set. For the main surface, we set the outer surface of the ring gear to the slave surface and set the contact properties to "Hard Contact" and "Penalty".

There are two loading steps in the simulation. In the first step, a slight magnitude of interference is set for the touching of the ring gear and gearbox, namely, $\delta_1 = 0.01$ mm. In the second step, the magnitude of interference between the ring gear and gearbox is the actual magnitude of interference. The two left and right sections are set as the periodic boundary condition, and the bottom of the ring gear touching the gearbox is set as the fixed boundary condition. The boundary conditions are shown in Figure 3.

4.4 Solution

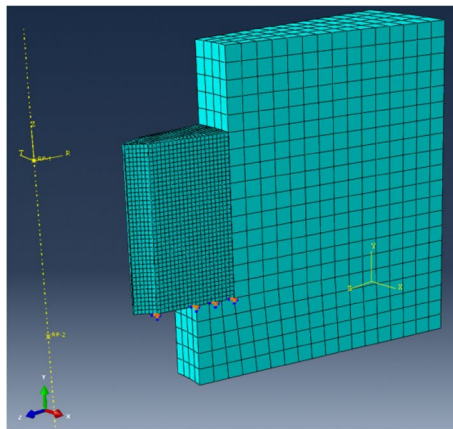
The tangential prestress σ_t of the inner ring interference is equal to the difference between the internal stress σ_n and the residual stress σ_c . The tangential prestressed cloud diagram of the inner ring of experiment 1 and experiment 8 is shown in Figure 4.



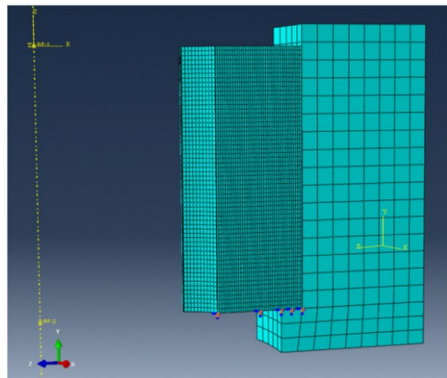
5 Experiment

At present, an XRD is the most mature method for measuring the residual surface stresses of a structure [25, 26]. The XRD method is a method for non-destructive measurement of stress. The area of XRD is small, so the size of the measurement point is also small, and the stress on the surface of the device to be tested can be measured within a few micrometers to several tens of micrometers, and it is more suitable for on-site measurement. The distance of the crystal face will change when internal stresses occur in a specimen. The diffraction peak will move with it when diffraction occurs. In addition, the displacement distance is related to the amount of internal stresses. The internal stresses can be calculated based on the displacement distance of the diffraction peak. The LXRDX-ray diffractometer, shown in Figure 5, was used in the experiment.

In this study, residual stresses occur in the specimens, and thus the residual stresses of the ring gear should first be measured. Then, nine groups of gearboxes are heated, and the gearboxes and ring gears are assembled together using a shrinkage and expansion assembly method. Finally, the prestressing of the ring gear is measured

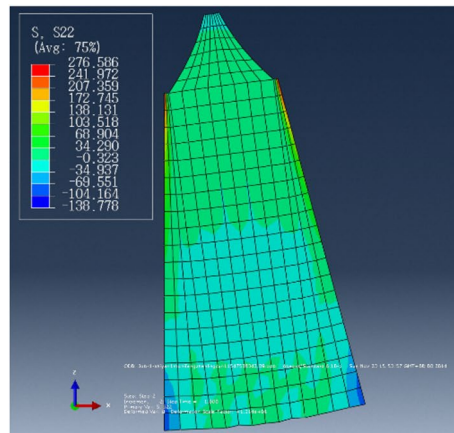


a Boundary conditions of experiment 1

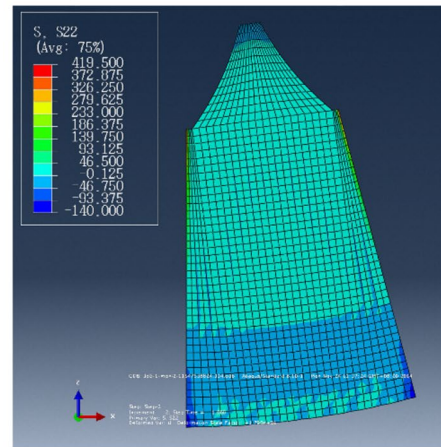


b Boundary conditions of experiment 8

Figure 3 Boundary conditions



a Equivalent stress cloud of experiment 1



b Equivalent stress cloud of experiment 8

Figure 4 Equivalent stress clouds of ring gear

using XRD. Experiments 1 and 8 are used as examples. In experiment 1, the gearbox is heated for 3 h at a temperature of 190 °C. In experiment 8, the gearbox is heated for 3 h at a temperature of 150 °C. Six measurement points are chosen in the specimen for experiment 1, and seven measuring points are chosen for the specimen in experiment 8. The measurement points are shown in Figure 6.

6 Comparison of the Results

According to the theoretical analysis, the simulation using ABAQUS, and the experimental method, the theoretical curves, simulation curves, and experimental curves of the prestressing of the ring gear in the interference fit for experiments 1 and 8 were chosen from the nine groups of experiments, and are shown in Figure 7.

Comparing the three curves in Figure 7, the errors in the simulation, experimental, and theoretical curves are less than 20%, and are attributed to postulated conditions, modeling, meshing, manufacturing error, and measurement errors.

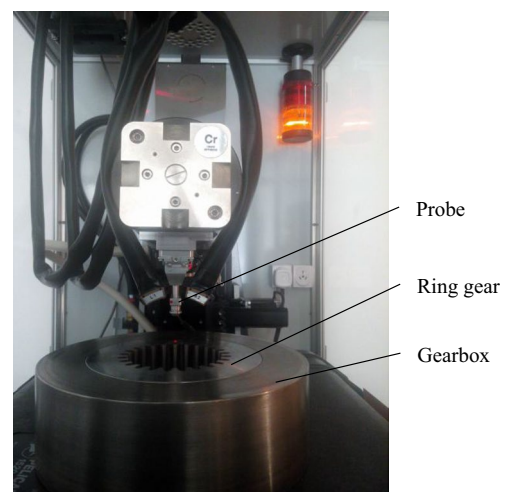
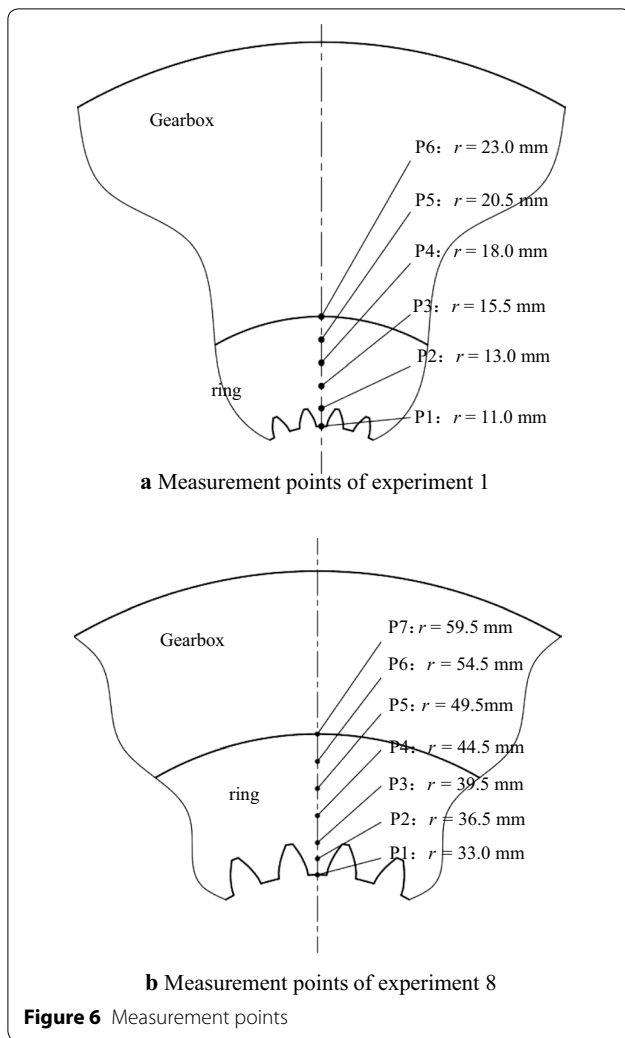
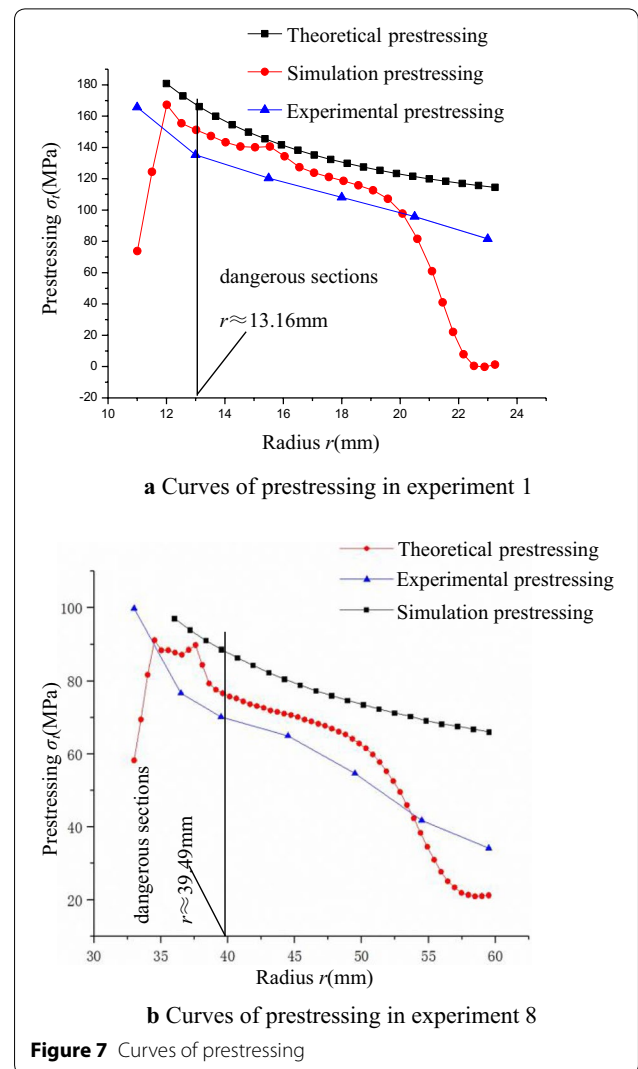


Figure 5 LXRD X-ray diffractometer



Based on an analysis of the nine groups of experiments, the actual prestressing value of the ring gear in an interference fit has certain differences with the theoretical value. The theoretical values are the highest, the simulation values are the second highest, and the experimental values are the lowest. To facilitate the design and calculation, the theory of prestressing is revised, and the correction coefficient of prestressing of the ring gear in interference fit Y_{Ia} is set when calculating the actual prestressing σ . As a result, the theoretical, simulation, and experimental values of the prestressing have different degrees of error. Their average values from the nine groups of experiments are first calculated, and compared with the theoretical value, and the correction coefficient of each experiment is then calculated. Finally, the correction coefficient of the prestressing of the ring gear in the interference fit is obtained by calculating the average value of nine groups of correction coefficient. As an



example of experiments 1 and 8, the calculated correction coefficients are listed in Tables 3 and 4.

The correction factor Y_{Ia1} in experiment 1 is obtained through calculations as $Y_{Ia1} = 0.893$. The correction factor Y_{Ia8} in experiment 8 is obtained through calculations as $Y_{Ia8} = 0.888$.

The nine groups of correction factors are obtained using the same method. The average correction factor is then calculated as $Y_{Ia} = 0.891$. Thus, the actual formula of the prestressing is as follows:

$$\sigma = Y_{Ia} \cdot \sigma_t = 0.891 \cdot \left(A_1 + B_1 \cdot \frac{1}{r^2} \right), \quad (6)$$

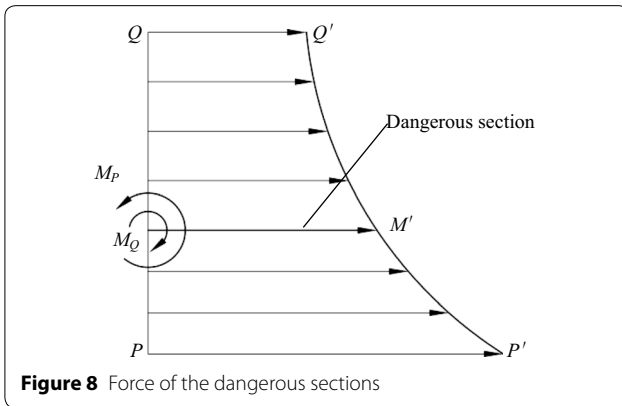
Eq. (6) can accurately calculate the prestressing of the inner ring gear in interference fit.

Table 3 Correction factors Y_{Ia1} in experiment 1

Radius r (mm)	Theoretical prestressing σ_1 (MPa)	Simulation prestressing σ_2 (MPa)	Experimental prestressing σ_3 (MPa)	Average prestressing σ_a (MPa)	Correction factor $Y_{Ia1} = \sigma_a/\sigma_1$
13.0	167.31	151.18	135.29	151.26	0.904
15.5	144.70	140.53	120.38	135.20	0.934
18.0	130.27	118.57	108.07	118.97	0.913
20.5	121.42	81.58	95.83	99.61	0.820

Table 4 Correction factors Y_{Ia8} in experiment 8

Radius r (mm)	Theoretical prestressing σ_1 (MPa)	Simulation prestressing σ_2 (MPa)	Experimental prestressing σ_3 (MPa)	Average prestressing σ_a (MPa)	Correction factor $Y_{Ia8} = \sigma_a/\sigma_1$
36.5	95.66	87.07	76.73	86.49	0.904
39.5	88.58	76.44	70.18	78.40	0.885
44.5	80.10	70.35	65.05	71.83	0.897
49.5	74.05	64.03	54.60	64.23	0.867



7 Correction Formula of the Tooth Root Flexural Fatigue Strength

When the gearbox body interference connects with the ring gear, a meshing load from the planet gears occurs, as does a prestressing, which is σ_t in the interference fit. The prestressing σ_p , which affects the dangerous sections MM' of the gear, can be decomposed into two bending moments M_P and M_Q , and stress σ_M . The force of the dangerous sections MM' is shown in Figure 8.

$$\begin{aligned}
 M_P &= \int_{r_P}^{r_M} \sigma dr = \int_{r_P}^{r_M} 0.891 \cdot \left(A_1 + B_1 \cdot \frac{1}{r^2} \right) dr \\
 &= 0.891 \cdot \left[A_1 \cdot r_M - B_1 \cdot \frac{1}{r_M} - \left(A_1 \cdot r_P - B_1 \cdot \frac{1}{r_P} \right) \right] \\
 &= 0.891 \cdot \left[A_1 \cdot (r_M - r_P) - B_1 \cdot \left(\frac{1}{r_M} - \frac{1}{r_P} \right) \right], \tag{7}
 \end{aligned}$$

$$\begin{aligned}
 M_Q &= \int_{r_M}^{r_Q} \sigma dr = \int_{r_M}^{r_Q} 0.891 \cdot \left(A_1 + B_1 \cdot \frac{1}{r^2} \right) dr \\
 &= 0.891 \cdot \left[A_1 \cdot r_Q - B_1 \cdot \frac{1}{r_Q} - \left(A_1 \cdot r_M - B_1 \cdot \frac{1}{r_M} \right) \right] \\
 &= 0.891 \cdot \left[A_1 \cdot (r_Q - r_M) - B_1 \cdot \left(\frac{1}{r_Q} - \frac{1}{r_M} \right) \right], \tag{8}
 \end{aligned}$$

$$\sigma_M = \frac{0.891 \cdot p \cdot r_Q^2}{r_Q^2 - r_P^2} \left(1 + \frac{r_P^2}{r_M^2} \right), \tag{9}$$

where $r_Q = r_i$ (radius of interface), $r_P = r_r$ (reference radius of ring gear), $r_M = \frac{S}{2 \tan(\gamma - \alpha)}$, the tooth thickness of the dangerous section is S [27, 28], the normal loading angle is γ , and the pressure angle is α .

Eqs. (7), (8), and (9) can be simplified as follows:

$$\begin{aligned}
 M_P &= 0.891A_1 \cdot \left[\frac{S}{2 \tan(\gamma - \alpha)} - r_r \right] \\
 &\quad - 0.891B_1 \cdot \left[\frac{2 \tan(\gamma - \alpha)}{S} - \frac{1}{r_r} \right], \tag{10}
 \end{aligned}$$

$$\begin{aligned}
 M_Q &= 0.891A_1 \cdot \left[r_i - \frac{S}{2 \tan(\gamma - \alpha)} \right] \\
 &\quad - 0.891B_1 \cdot \left[\frac{1}{r_i} - \frac{2 \tan(\gamma - \alpha)}{S} \right], \tag{11}
 \end{aligned}$$

$$\sigma_M = \frac{0.891 \cdot p \cdot r_i^2}{r_i^2 - r_r^2} \left[1 + \frac{4r_r^2 \cdot \tan^2(\gamma - \alpha)}{S^2} \right]. \quad (12)$$

In a traditional gear bending fatigue strength calculation, when the ring gear is loaded, the bending stress of the dangerous sections of the single tooth is shown as below:

$$\begin{aligned} \sigma_{F0} &= \frac{M}{W} = \frac{p_{ca} \cdot \cos \gamma \cdot h}{\frac{1 \times S^2}{6}} \\ &= \frac{6p_{ca} \cdot \cos \gamma \cdot h}{S^2}, \end{aligned} \quad (13)$$

where the meshing load is p_{ca} .

Therefore, the bending stress produced by the two bending moments, M_P and M_Q , in the dangerous sections is shown below [29, 30]:

$$\begin{aligned} \sigma_I &= \frac{M_P - M_Q}{W} = \frac{M_P - M_Q}{\frac{1 \times S^2}{6}} \\ &= \frac{5.346A_1}{S \cdot \tan(\gamma - \alpha)} - \frac{21.384B_1 \tan(\gamma - \alpha)}{S^3} \\ &\quad - \frac{5.346A_1(r_r + r_i)}{S^2} + \frac{5.346B_1 \left(\frac{1}{r_r} + \frac{1}{r_i} \right)}{S^2}. \end{aligned} \quad (14)$$

Finally, the correction formula of the tooth root flexural fatigue strength is obtained as

$$\begin{aligned} \sigma'_F &= \sigma_{F0} + \sigma_I + \sigma_M = \frac{KF_t Y_{Fa} Y_{Sa}}{bm} + \frac{5.346A_1}{S \cdot \tan(\gamma - \alpha)} \\ &\quad - \frac{21.384B_1 \tan(\gamma - \alpha)}{S^3} - \frac{5.346A_1(r_r + r_i)}{S^2} \\ &\quad + \frac{0.891p \cdot r_i^2}{r_i^2 - r_r^2} \left[1 + \frac{4r_r^2 \cdot \tan^2(\gamma - \alpha)}{S^2} \right] \\ &\quad + \frac{5.346B_1 \left(\frac{1}{r_r} + \frac{1}{r_i} \right)}{S^2} \leq [\sigma_F]. \end{aligned} \quad (15)$$

8 Conclusions

- (1) Based on the method for calculating the prestressing of a thick cylinder in an interference fit, the ring gear is equivalent to a thick cylinder, and the mathematical model of prestressing of the ring gear in the interference fit is developed. The distribution rule of prestressing is inferred.
- (2) Through theoretical calculation, simulation, and XRD measurements, nine groups of theoretical curves, simulation curves, and experimental curves

for a prestressing of the ring gear in the interference fit are obtained. In the contrasting results of the three curves, the theoretical values are the highest, the simulation values are second highest, and the experimental values are the lowest. To facilitate the design, a theoretical calculation method of prestressing is adopted. The theoretical values are larger than the actual values, and thus the theoretical values should be corrected. The correction factor of prestressing of the ring gear in an interference fit was obtained using a contrast calculation. The correction factor $Y_{Ia} = 0.891$ can be used to accurately calculate the prestressing of the inner ring gear of the interference connection, and provides a theoretical method for calculating the prestressing of the spur gear ring.

- (3) The stress of the ring gear in the meshing and the prestressing of the ring gear in the interference fit are composed. The final correction formula of the tooth root flexural fatigue strength is obtained. It provides theoretical guidance for practical design and production.

Authors' Contributions

SY was in charge of the whole trial; SY and YJ wrote the manuscript; YM and TX assisted with sampling and laboratory analyses. All authors read and approved the final manuscript.

Authors' Information

Shiping Yang, born in 1970, is currently a professor at *Xiangtan University, China*. He received his PhD degree from *Xiangtan University, China*, in 2014. His research interests include Gear dynamics and Spatial multiple conjugate transmission.

Yixing Ji, born in 1992, is currently working towards a master's degree in engineering at *School of Mechanical Engineering, Xiangtan University, China*.

Yulin Mo, born in 1989, graduated from *Xiangtan University, China*, now is freelance.

Tianyu Xia, born in 1993, graduated from *Xiangtan University, China*, now is freelance.

Competing Interests

The authors declare that they have no competing interests.

Funding

Supported by Hunan Provincial Natural Science Foundation of China (Grant No. 2018JJ4006) and National Independent Innovation Demonstration Area Foundation of Changsha Zhuzhou Xiangtan (Grant No. 2018XK2302).

Received: 12 June 2018 Accepted: 7 August 2019

Published online: 20 August 2019

References

- [1] Standardization Administration of the People's Republic of China. GB/T 5371-2004 Rules for content, limits and fits-the calculation and selection of interference fits. Beijing: *China Standard Publishing House*, 2004. (in Chinese)

- [2] German Institute of Standardization. DIN7190-2001 Rules for content, interference fits-calculation and design rules. Germany: *German Institute of Standardization*, 2001.
- [3] Iglesias Miguel, Fernández Del Rincón Alfonso, De-Juan Ana Magdalena, et al. Planetary gear profile modification design based on load sharing modelling. *Chinese Journal of Mechanical Engineering*, 2015, 28(4): 810–820.
- [4] X Y Xu, C C Zhu, H J Liu, et al. Load sharing research of planetary gear transmission system of wind turbine gearbox with flexible pins. *Journal of Mechanical Engineering*, 2014, 50(11): 43–49. (in Chinese)
- [5] H Zhu, W Cheng, G H Jia, et al. Dynamic performance simulation on wind-power pitch planetary reducer. *Journal of Central South University (Science and Technology)*, 2011, 10 (42): 3059–3065. (in Chinese)
- [6] Y J Jiang. The calculation of prestresses of the ring in the thermal-coordinated gear. *Inner Mongolia Science Technology and Economy*, 2005, 5: 105–106. (in Chinese)
- [7] Y Zou, F C Sun, W Q Wang, et al. Study on the relation between gear's hole diameter and prestressing force in interference fit. *Journal of Mechanical Transmission*, 2003, 27(6): 41–42. (in Chinese)
- [8] X Y Yan, C X Hong, H Liu, et al. Prestresses of the ring in the thermal-coordinated gear. *Journal of Electric Power*, 1994, 9(2): 6–10. (in Chinese)
- [9] C Q Zhu. Prestress analysis of keyless connection sleeve in hot assembly based on ANSYS. *Shandong Metallurgy*, 2013, 35(4): 70–72. (in Chinese)
- [10] L Zhao, H C Wu, L M Zhao, et al. Prestressed mode analysis of planetary gear train in automatic hydraulic transmission based on ANSYS. *Mechanical Engineer*, 2015, (08): 31–33. (in Chinese)
- [11] G F Wang. Analysis of Influence of prestressing on interference fit of dump truck axle. *Internal Combustion Engine & Parts*, 2018, (16): 65–67. (in Chinese)
- [12] H Y Kim, C Kim, W B Bae. Development of optimization technique of warm shrink fitting process for automotive transmission parts (3D FE analysis). *Journal of Materials Processing Technology*, 2007, 187: 458–462.
- [13] Rahman Seifi, Kaveh Abbasi. Friction coefficient estimation in shaft/bush interference using finite element model updating. *Engineering Failure Analysis*, 2015, 57: 310–322.
- [14] D S Hao, D L Wang. Finite-element modeling of the failure of interference-fit planet carrier and shaft assembly. *Engineering Failure Analysis*, 2013, 33: 184–196.
- [15] Frederic Lanoue, Aurelian Vadean, Bernard Sanschagrín. Fretting fatigue strength reduction factor for interference fits. *Simulation Modelling Practice and Theory*, 2011, 19: 1811–1823.
- [16] X Q Xu, H H Zhao. Nonlinear FEM analysis of the contact stress on interference fitting surfaces. *Machine Design and Research*, 2000, (1): 33–35. (in Chinese)
- [17] Y Zhang, B McClain, X D Fang. Design of interference fits via finite element method. *International Journal of Mechanical Sciences*, 2000, 42: 1835–1850.
- [18] L Amanan, K R Krishna, R Sriraman. Thermo-mechanical finite element analysis of a rail wheel. *International Journal of Mechanical Sciences*, 1999, 41: 487–505.
- [19] Z B Wang. *Research on lightweight design technology for large scale yaw and pitch gearboxes*. Zhengzhou: Zhengzhou Machinery Research Institute, 2012. (in Chinese)
- [20] Z H Zhang, Z M Liu, H P Zhang, et al. The structural analysis of single planet carrier for yaw and pitch gearbox. *Journal of Mechanical Engineering*, 2012, 48(6): 68–70. (in Chinese)
- [21] L G Pu, G D Chen. *Design of machinery*. Beijing: Higher Education Press, 2012. (in Chinese)
- [22] D Q Xu, R W Sun. *The design, calculation, assembly and disassembly of the interference fit*. Beijing: China Metrology Press, 1992. (in Chinese)
- [23] R J Teng, Y B Zhang, X J Zhou, et al. Mechanical properties and design method of cylindrical interference fit. *Journal of Mechanical Engineering*, 2012, 48(13): 160–166. (in Chinese)
- [24] Z X Liu, L Wang. *Experimental design & data processing*. Beijing: Chemical Industry Press, 2015. (in Chinese)
- [25] T H Zhang, Y Wang, X F Fang, et al. Research status and development of residual stress detection and elimination methods. *Journal of Netshape Forming Engineering*, 2017, 9(5): 122–127. (in Chinese)
- [26] Ines Fernandez Pariente, Mario Guagliano. Contact fatigue damage analysis of shot peened gears by means of X-ray measurements. *Engineering Failure Analysis*, 2009, 16: 964–971.
- [27] Standardization Administration of the People's Republic of China. GB/T 3480.5-2008 Rules for content, calculation of load capacity of spur and helical gears-part 5: strength and quality of materials. Beijing: China Standard Publishing House, 2008. (in Chinese)
- [28] Vincent Savaria, Florent Bridier, Philippe Bocher. Predicting the effects of material properties gradient and residual stresses on the bending fatigue strength of induction hardened aeronautical gears. *International Journal of Fatigue*, 2016, 85(4): 70–84.
- [29] Gabriel Marsh, Colin Wignall, Philipp R Thies, et al. Review and application of Rainflow residue processing techniques for accurate fatigue damage estimation. *International Journal of Fatigue*, 2016, 82(3): 757–765.
- [30] Mir Ali Ghaffari, Eric Pahl, Shaoping Xiao. Three dimensional fatigue crack initiation and propagation analysis of a gear tooth under various load conditions and fatigue life extension with boron/epoxy patches. *Engineering Fracture Mechanics*, 2015, 135: 126–146.

Submit your manuscript to a SpringerOpen[®] journal and benefit from:

- Convenient online submission
- Rigorous peer review
- Open access: articles freely available online
- High visibility within the field
- Retaining the copyright to your article

Submit your next manuscript at ► [springeropen.com](https://www.springeropen.com)
